

# Mechanochemical and Thermal Transformations of Amorphous and Crystalline Aluminosilicates

KUI – 1/2007  
Received May 30, 2006  
Accepted September 7, 2006

C. Kosanović and B. Subotić

Ruder Bošković Institute, Bijenička 54, 10000 Zagreb, Croatia  
E-mail: cleo@irb.hr, subotic@irb.hr

Preparation of amorphous aluminosilicates precursors with defined properties is a very important factor for further studies of nucleation and crystal growth of zeolites during their thermal and hydrothermal transformation into zeolites and special ceramics. This study presents the effect of an intensive mechanical force (ball-milling) on the properties of zeolite A and zeolite A with partially exchanged sodium ions with other cations ( $\text{Li}^+$ ,  $\text{K}^+$ ,  $\text{Cs}^+$ ,  $\text{NH}_4^+$ ). The influence is studied of different cations on the mechanical and thermal stability of the zeolite framework and the formation of amorphous phases, as well as their transformation into nonzeolitic crystal phases after thermal treatment.

Keywords: Zeolites, ball-milling, cation exchange, temperature-induced transformations

## Introduction

Zeolites or molecular sieves are hydrated crystalline aluminosilicates with a unique open framework structure consisting of  $\text{SiO}_4$  and  $\text{AlO}_4$  tetrahedra (primary building units) linked by common oxygen atoms,<sup>1</sup> as schematically presented in Fig. 1.

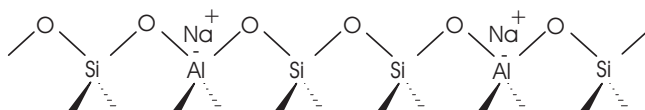


Fig. 1 – Schematic of linking of the primary building units ( $\text{TO}_4$ ) in zeolites,  $T = \text{Si}$  or  $\text{Al}$

Slika 1 – Shematski prikaz povezivanja primarnih jedinica građe ( $\text{TO}_4$ ) u zeolitima;  $T = \text{Si}$  ili  $\text{Al}$

In reality, the primary building units do not form simple chain structures (see Fig. 1), but rather more complex two- and three-dimensional structures, so-called secondary building units (SBU; see Fig. 2), which combination results in the formation of a three-dimensional framework, characteristic for a given type of zeolite.

Specific linkages of the primary and secondary building units result in the formation of the channels and/or cages (cavities) interconnected by “windows” and channels.<sup>1–5</sup> The size and shape of “windows”, channels and cages, as well as their mutual positions in the zeolite framework are known and constant for a given type of zeolite, and thus represent its structural particularity.<sup>1–6</sup>

The chemical composition of zeolites is generally represented by the formula:  $\text{Me}_{2/n}\text{O} \cdot \text{Al}_2\text{O}_3 \cdot x\text{SiO}_2 \cdot y\text{H}_2\text{O}$ , where Me is hydrated cation that compensates the negative char-

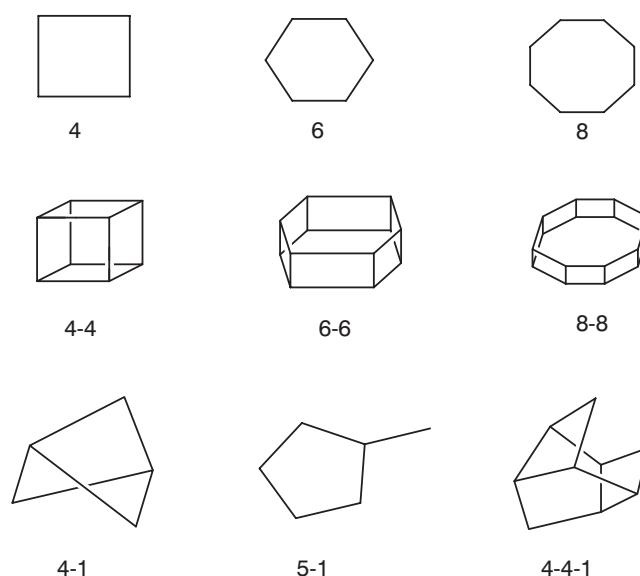


Fig. 2 – Secondary building units (SBU). Numbers symbolically denote chemical bonds in planar and polyhedral structural units of zeolites

Slika 2 – Sekundarne jedinice građe zeolita (SBU). Brojke simbolički označavaju kemijske veze u planarnim i poliedarskim strukturnim jedinicama zeolita

ge of the framework (see Fig. 1),  $n$  is the charge of the compensating cation,  $x \geq 2$  depends on the type of zeolite and is determined by Lowenstein's rule,<sup>7</sup> while  $y$  is determined by both the type of zeolite and the nature of the compensating cation.<sup>1,4,5</sup>

The properties of zeolites such as ion exchange, intercrystalline pores that discriminate between molecules of diffe-

rent dimensions, strong acidic sites and active hosts for metal catalyzed reactions have earned them extensive industrial uses, and zeolite research has become an area of considerable interest.<sup>2,8,9</sup> The interest in the use of zeolites as catalysts, adsorbents and detergent builders has grown in the last three decades.<sup>9</sup> Millions of tons of zeolite 4A are used annually in the detergent industry, hundreds of thousands tons in the petroleum processing industry alone, while their use in other areas is still in a stage of infancy.<sup>9–11</sup> Success on such a large scale and the possibility of synthesizing novel zeolites has made zeolite synthesis an actively researched area in many academic and industrial laboratories.

One very attractive and promising area of zeolite research is that of obtaining new materials by thermal treatment of different types of zeolites modified by ion exchange. Thus, the thermal transformation of zeolite precursors is a novel route for the synthesis of aluminosilicate-based ceramics,<sup>12</sup> which has found numerous applications in the ceramic industry.<sup>13</sup> In addition, recent investigations have shown that not only zeolites, but also amorphous aluminosilicates both form by precipitation,<sup>14</sup> and that the amorphous phase obtained by mechanical treatment of zeolites<sup>15,16</sup> can be transformed into aluminosilicate-based ceramics. For this reason, the objective of this work is to show the influence of the mechanical treatment of zeolites on their properties relevant for the use of zeolites as precursors in the preparation of aluminosilicate-based ceramics.

## Experimental

Zeolite Linde 4A ( $\text{Na}_2\text{O} \cdot \text{Al}_2\text{O}_3 \cdot 2\text{SiO}_2 \cdot 4\text{H}_2\text{O}$ ; prepared in our laboratory by a known procedure) was used as starting material.

Partial exchange of original  $\text{Na}^+$  ions from zeolite 4A with  $\text{Li}^+$ ,  $\text{K}^+$ ,  $\text{Cs}^+$  and  $\text{NH}_4^+$  ions from solution was carried out as follows:

10 g of powdered zeolite A was placed in a stainless steel reaction vessel containing 250 ml of  $C = 0.5 \text{ mol dm}^{-3}$  solution of MeCl (where Me =  $\text{Li}^+$ ,  $\text{K}^+$ ,  $\text{Cs}^+$  and  $\text{NH}_4^+$  ion) preheated at  $T = 80^\circ\text{C}$ . The suspension was stirred 1 h at  $80^\circ\text{C}$ , and thereafter the solid phase was separated from the solution by filtration. The residue on the filter paper was redispersed in a fresh 250 ml portion of  $C = 0.5 \text{ mol dm}^{-3}$  solution of potassium chloride and stirred again for 1 h at  $80^\circ\text{C}$ . The exchange and separation procedure was carried out three times in all. After final solid/liquid separation, the residue on the filter paper was rinsed with distilled water until the reaction of the filtrate with  $\text{AgNO}_3$  yielded a negative result, and then dried at  $105^\circ\text{C}$  for 24 h. The exchanged zeolites were kept in a desiccator with saturated NaCl solution for 24 h before analysis.

Chemical composition of the exchanged zeolite was determined as follows: A given amount (about  $m = 15 \text{ mg}$ ) of the solid was dissolved in 1 ml of concentrated  $\text{HNO}_3$ , and then the solution was diluted with distilled water to the concentration ranges available for measuring the concentrations of silicon, sodium and potassium ions by atomic absorption spectroscopy. To determine the aluminium content in the exchanged zeolite, about  $m = 15 \text{ mg}$  of solid

was dissolved in 1 ml of concentrated HF, and then the solution was heated in order to remove silicon by offgassing the  $\text{SiF}_4$ . The solution was diluted with distilled water to the concentration ranges available for measuring the concentration of aluminium, sodium and potassium ions by atomic absorption spectroscopy. The concentration of silicon, aluminium, and sodium and potassium ions in the solutions obtained by the dissolution of the solids were measured by the Shimadzu AA-660 atomic absorption/flame emission spectrophotometer. Water content the solid samples was determined from the corresponding TG (thermogravimetry) curves.

The samples of hydrous zeolites 4A, as well as the samples obtained by partial exchange of  $\text{Na}^+$  ions from zeolite 4A with  $\text{Li}^+$ ,  $\text{K}^+$ , and  $\text{Cs}^+$  ions from the solution were milled in a planetary ball mill (Fritsch Pulverisette type 7) at room temperature. For this purpose, a certain amount of each sample was put in an agate vessel containing 10 wolfram carbide balls ( $d = 10 \text{ mm}$ ), and then the vessel was rotated (speed of rotation was  $n = 3000 \text{ min}^{-1}$ ) until the crystalline starting powder had been completely transformed into X-ray amorphous material. The samples amorphized by ball-milling were kept in a desiccator with saturated NaCl solution for 24 h before analysis.

The samples obtained after cation exchanging and ball-milling, as well the samples of the original exchanged zeolite A with  $\text{Li}^+$ ,  $\text{K}^+$ ,  $\text{Cs}^+$  and  $\text{NH}_4^+$  ions, were heated at appropriate temperatures in a chamber furnace with controlled temperature (ELPH-2, Elektrosanitarij).

Differential thermogravimetry (DTG) and differential scanning calorimetry (DSC) of the samples were done by a Netzsch STA 409 simultaneous thermal analysis apparatus. The samples were heated in a platinum crucible ( $d = 6.8 \text{ mm}$ ,  $l = 2.6 \text{ mm}$ ) at a heating rate of  $\Delta T = 10 \text{ K min}^{-1}$  in a nitrogen atmosphere. The flow rate of nitrogen was  $15 \text{ cm}^3 \text{ min}^{-1}$ . About 30 mg of the sample was used in each run. Calcined kaolin was used as a reference.

The processes of amorphization, cation exchanging, and thermal treatment were followed by powder X-ray diffraction (Philips PW 1820 vertical goniometer with  $\text{CuK}$  graphite radiation).

The scanning electron micrographs of the samples were taken by Philips SEM 515.

## Results of mechanical and combined (mechanical + thermal) treatment of zeolites

The study of the influence of mechanical treatment (ball-milling) on the physicochemical properties of zeolite A, and zeolite A with the  $\text{Na}^+$  ions partly exchanged by  $\text{Li}^+$ ,  $\text{K}^+$ ,  $\text{Cs}^+$  and  $\text{NH}_4^+$  ions, showed that mechanical treatment causes the change of particulate properties of zeolites (Fig. 3) followed by the loss of crystallinity and the formation of X-ray amorphous samples having the same chemical composition as the original crystalline zeolites.<sup>15,17,18</sup> Analyses of the changes in X-ray diffraction (XRD) patterns and infrared (IR) spectra of the solid samples obtained at different stages of zeolite ball-milling indicated that amorphization (formation of X-ray amorphous phases) is caused by breaking

Si-O-Si and Si-O-Al bonds of the zeolite framework structure under the action of strong mechanical forces, and thus that such a process leads to the formation of "true" amorphous aluminosilicate phases with physicochemical properties similar to the precipitated amorphous aluminosilicates.<sup>15,17,18</sup> These indications are supported by the increased solubility of the milled samples in the alkaline solutions. By the same principle, the observed decrease of the cation-exchange capacity during milling is explained by the destruction of the original hole-channel structure of the zeolite and by blocking most of the exchangeable cations ( $\text{Na}^+$ ) inside the newly formed amorphous phase.<sup>15</sup>

The scanning-electron micrographs in Fig. 3 show that a starting short-term milling causes comminution of the original crystals (a) by their breakage and damage under the action of an intensive mechanical force; (b) part of the smaller particles forms aggregates with a marked irregular shape during further milling, as shown in Fig. 3b.

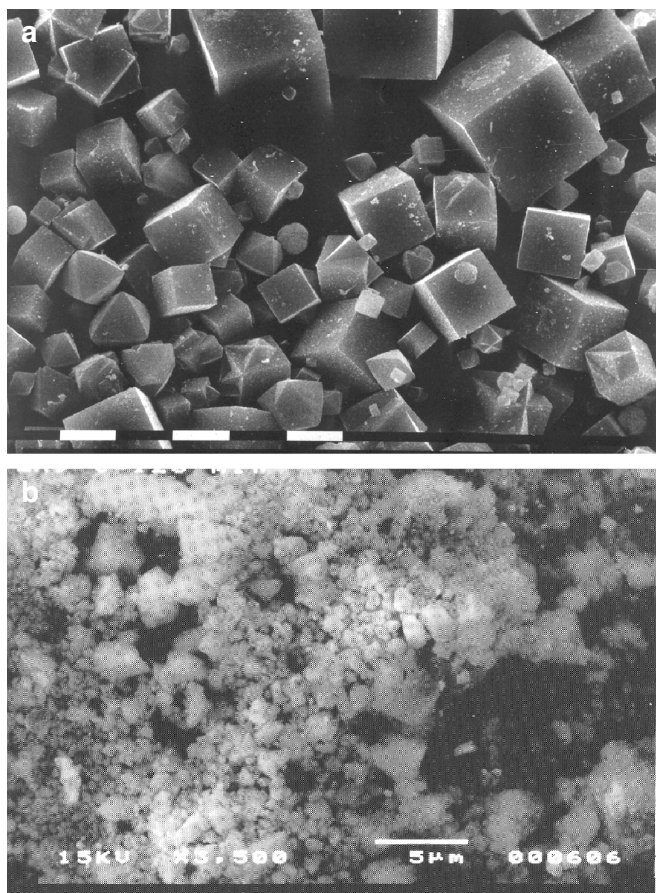


Fig. 3 – Scanning-electron micrographs of (a) zeolite A and (b) zeolite A after ball-milling

Slika 3 – Pretražne elektronske mikrofografije (a) zeolit A i (b) zeolit A nakon mljevenja u kugličnom mlinu

Kinetic analysis of the amorphization of the original and exchanged zeolite A showed that the change in fraction  $w_a$  of the amorphous phase obtained during ball-milling of exchanged zeolites can be expressed by differential equation:<sup>15</sup>

$$r_a = dw_a/dt_m = k(1 - w_a) \quad (1)$$

where  $t_m$  is milling time and  $k$  is the rate coefficient. The value of  $k$  generally depends on the milling conditions (speed of rotation, number of balls, and amount of treated material). Integration of Eq. (1) gives:

$$w_a = 1 - \exp(-k t_m) \quad (2)$$

The corresponding numerical values of  $k$  are calculated from the slopes of the straight lines obtained by plotting  $\ln(1 - w_a)$  versus  $t_m$ .<sup>15,19</sup>

Exchange of original sodium ions from zeolite A with other cations ( $\text{Li}^+$ ,  $\text{K}^+$ ,  $\text{Cs}^+$ ; see Table 1) from the solution (changes neither the basis structure of zeolite A nor the unit cell parameters, as revealed by X-ray powder diffractometry and FTIR spectroscopy.<sup>19</sup>

Table 1 – Chemical compositions of the original and exchanged zeolites used as precursors in thermal and mechanochemical treatment. The chemical composition is expressed as the amount of constitutive oxides ( $\text{Na}_2\text{O}$ ,  $\text{R}_2\text{O}$ ,  $\text{SiO}_2$ ,  $\text{H}_2\text{O}$ ) per amount of  $\text{Al}_2\text{O}_3$  in accordance with the oxide compositions of the zeolites:  $(x_1\text{Na}_2\text{O}, x_2\text{R}_2\text{O}) \cdot \text{Al}_2\text{O}_3 \cdot y\text{SiO}_2 \cdot z\text{H}_2\text{O}$

Table 1 – Kemijski sastav izvornih i zamijenjenih zeolita korištenih kao prekursori u termičkoj i mehanokemijskoj obradi. Kemijski sastav je izražen kao množina sastavnih oksida ( $\text{Na}_2\text{O}$ ,  $\text{R}_2\text{O}$ ,  $\text{SiO}_2$ ,  $\text{H}_2\text{O}$ ) po množini  $\text{Al}_2\text{O}_3$  prema oksidnom sastavu zeolita:  $(x_1\text{Na}_2\text{O}, x_2\text{R}_2\text{O}) \cdot \text{Al}_2\text{O}_3 \cdot y\text{SiO}_2 \cdot z\text{H}_2\text{O}$

Type of zeolite Vrste zeolita	$x_1$	$x_2$	$y$	$z$
NaA	1	-	2	4.5
(Li,Na)A	0.36	0.64	2	3.82
(K,Na)A	0.22	0.78	2	3.48
(Cs,Na)A	0.66	0.34	2	2.98
( $\text{NH}_4$ ,Na)A	0.21	0.79	2	4.15

$\text{R}_2\text{O} = \text{Li}_2\text{O}, \text{K}_2\text{O}, \text{Cs}_2\text{O}$  and  $(\text{NH}_4)_2\text{O}$

The slight lowering of the cell constant in the case of zeolite A with  $\text{Na}^+$  ions partly exchanged by  $\text{Li}^+$  ions (Table 2) was explained by the distortion of the zeolite framework caused by strong electrostatic interaction between the zeolite framework and the small, strongly polarizing  $\text{Li}^+$  ion.<sup>19–22</sup>

Table 2 – Cell constant  $a$  of zeolite A in which part of the sodium ions was exchanged with other cations ( $\text{R}^+$ ).  $k$  is the rate coefficient in Eq. (1) and Eq. (2), respectively, and  $f_R$  is the fraction of cation  $\text{R}^+$  in the framework of zeolite A

Table 2 – Konstante  $a$  jedinične ćelije zeolita A u kojem je dio natrijevih iona zamijenjen drugim kationima ( $\text{R}^+$ ).  $k$  je koeficijent u jednačbama (1) i (2) a  $f_R$  je udjel kationa  $\text{R}^+$  u strukturi zeolita A

Cation, $\text{R}^+$ Kation, $\text{R}^+$	$f_R$	$a$ (Å)	$k/\text{h}^{-1}$
$\text{Li}^+$	0.64	12.055	1.32
$\text{Na}^+$	1.0	12.308	3.82
$\text{K}^+$	0.78	12.276	9.85
$\text{Cs}^+$	0.34	12.332	19.51
$\text{NH}_4^+$	0.79	12.324	12.25

As expected from the invariability of the cell parameters of zeolite A (see Table 2), partial exchange of sodium with  $\text{Li}^+$ ,  $\text{K}^+$  and  $\text{Cs}^+$  ions does not affect the basic mechanism of the amorphization process; in all the cases, the kinetics of amorphization can be described by Eq. (1) and Eq. (2), respectively, as revealed by satisfying correlations between the measured and calculated values of  $w_a$  (see Fig. 4).<sup>19</sup> On the other hand, the rate of amorphization considerably depends on the type of cation (see Fig. 4).<sup>19</sup> Assuming that the breakage of Si–O–Si and Si–O–Al bonds of the zeolite framework structure can be reduced by decreasing the “empty” space in the zeolite framework, i.e., by increasing the volume  $V_{oc}$ , occupied in the unit cell of zeolite by cation,<sup>19</sup> the decrease of the rate of amorphization in the sequence:  $R(\text{Na}^+) > R(\text{Na}^+, \text{K}^+) > R(\text{Na}^+, \text{Cs}^+) > R(\text{Na}^+, \text{NH}_4^+)$  can be explained by the increase of volume  $V_{oc}$  in the sequence:  $V_{oc}(\text{Na}^+) < V_{oc}(\text{Na}^+, \text{K}^+) < V_{oc}(\text{Na}^+, \text{Cs}^+) < V_{oc}(\text{Na}^+, \text{NH}_4^+)$ .<sup>19</sup> In other words, the hydrated cations occupying the voids and channels in the zeolite structure compensate the strong exterior mechanical force, thus decreasing the rate of amorphization by mechanical stabilization of the zeolite framework structure. Of course, the extent of stabilization depends on the nature of the cation including the charge and degree of hydration, as well as on the extent of exchange. In this context,  $R(\text{Na}^+) > R(\text{Na}^+, \text{Li}^+)$  for  $V_{oc}(\text{Na}^+, \text{Li}^+) < V_{oc}(\text{Na}^+)$  can again be explained by the strong polarization of  $\text{Li}^+$  ion.

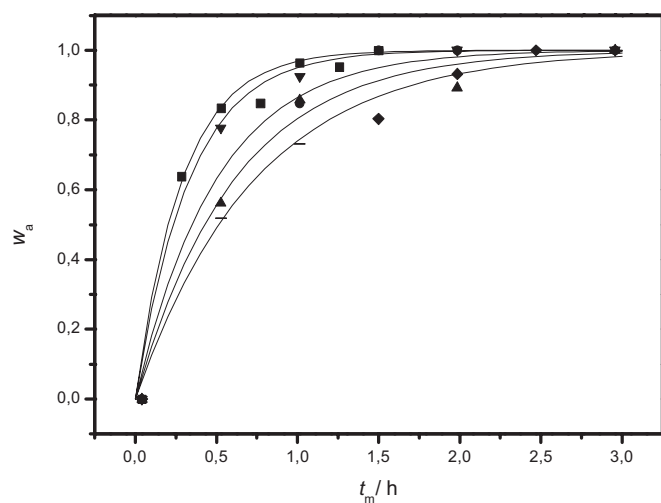


Figure 4 – Changes of the fraction,  $w_a$ , of X-ray amorphous phase in the samples obtained by ball-milling the sodium form of zeolite A (■), and zeolite A with partially exchanged  $\text{Na}^+$  ions by  $\text{Li}^+$  (▼),  $\text{K}^+$  (▲),  $\text{Cs}^+$  (●) and  $\text{NH}_4^+$  (◆). The curves represent the  $w_a$  vs.  $t_m$  functions calculated by Eq. (2) using the corresponding values of  $k$  (Table 2)

Slika 4 – Promjena udjela,  $w_a$ , rendgenski amorfnе faze u uzorcima dobivenom mljevenjem natrijeve forme zeolita A (■) i zeolita u kojem je dio iona  $\text{Na}^+$  zamijenjen s  $\text{Li}^+$  (▼),  $\text{K}^+$  (▲),  $\text{Cs}^+$  (●) i  $\text{NH}_4^+$  (◆). Krivulju pokazuju ovisnosti  $w_a$  o  $t_m$  izračunate pomoću jednadžbe (3) i odgovarajućih vrijednosti koeficijenta  $k$  (Tablica 2)

Taking into consideration the drastic structural changes of the zeolite framework during its mechanochemical treatment<sup>15,17,18</sup> and the influence of the cations on the observed changes,<sup>19</sup> it was assumed that the mechanochemical amorphization of zeolites changes the interactions between

the cations and the aluminosilicate matrix of the treated zeolites, and thus the mechanism and kinetics of dehydration. Thermal analysis has frequently been used for the study of dehydration of different minerals including zeolites and clays.<sup>23–25</sup> The results of the simultaneous thermal analysis are very sensitive to the nature of the cations present in the aluminosilicate environment and to the interactions of the cations with the zeolite framework. It can give useful information about the pore structure, catalytic activity, degree of hydration of the cations and their interactions with the aluminosilicate matrix of zeolites and amorphous aluminosilicates.<sup>26–28</sup> Fig. 5A shows the results of thermogravimetric analysis of zeolite A partly exchanged sodium ions with other cations ( $\text{Li}^+$ ,  $\text{K}^+$ ,  $\text{Cs}^+$ ), and Fig. 5B shows the results of thermogravimetric analysis of the samples obtained by ball-milling of the above-mentioned zeolites. The largest rate of dehydration (dotted curve in Fig. 5A), and consequently, the lowest temperature of dehydration ( $T \approx 130$  °C)<sup>13</sup> of cesium-exchanged zeolite A are consequences of the weak electrostatic interaction between the cesium ion and the water molecules.<sup>29, 30</sup>

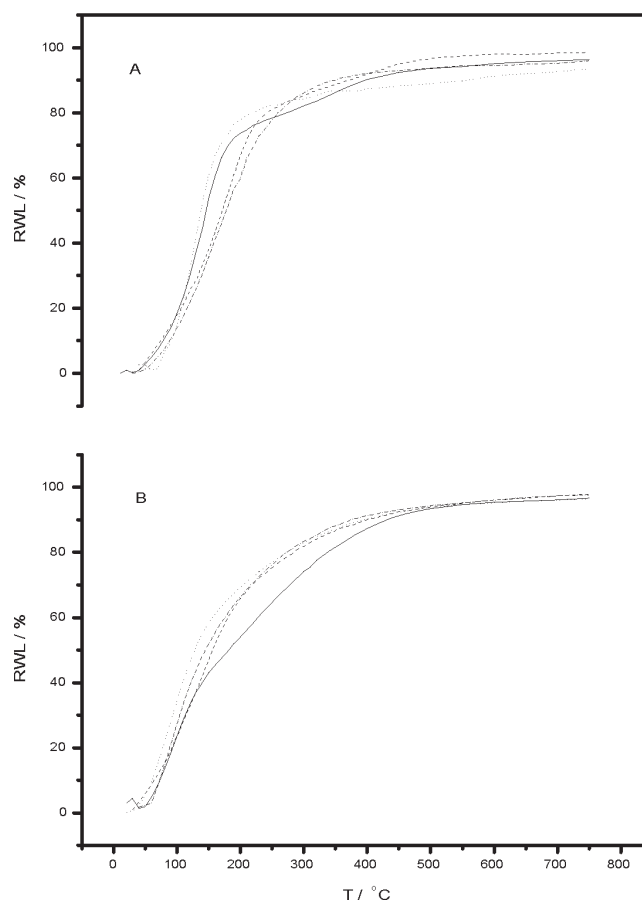


Fig. 5 – Relative loss of mass, RLW, during the controlled heating of the original crystalline (A) and the amorphized (B) samples of zeolite A with the original sodium ions partly exchanged by  $\text{Li}^+$  (solid curve),  $\text{K}^+$  (dashed-dotted curve) and  $\text{Cs}^+$  ions (dotted curve). The dashed curves corresponds to the RLW of the original (A) and amorphized (B) samples of zeolite A (Na-form).

Slika 5 – Gubitak mase uzrokovan desorpcijom vode tijekom grijanja zeolita A i zeolita A u kojem je dio originalnih  $\text{Na}^+$  iona zamijenjen s  $\text{Li}^+$  (—),  $\text{K}^+$  (— · —),  $\text{Cs}^+$  (···) ionima (A) uzoraka istih zeolita dobivenih mljevenjem (B). Crtkane krivulje (---) odgovaraju gubitku mase izvornog zeolita A (A) i amorfne uzorak zeolita A (B) (u Na-obliku).

“Reprinted from Publication printed in *Thermochemica acta*, 276, Authors: C. Kosanović, B. Subotić and A. Čížmek, pages 91–103, Copyright (1996), with permission from Elsevier”.

On the other hand, despite strong electrostatic interaction between lithium ions and water molecules,<sup>31</sup> the relatively high rate of dehydration of the sample in which part of the sodium ions was exchanged with smaller lithium ions (solid curve in Fig. 5A), leads to an assumption that a larger amount of energy is spent on the diffusion of water molecules through the channel/void system of the zeolite structure than on the dehydration of the hydrated lithium ions. In this context, the decrease of the dehydration rate in the sequence:  $r_{d,Na,Cs} > r_{d,Na,Li} > r_{d,Na} > r_{d,Na,K}$  (see Fig. 5A) is logical and expected, taking into consideration the different size, degree of hydration, and degree of exchange.<sup>16</sup>

The “true” amorphous phases obtained by ball-milling zeolites have a system of micro-, meso- and macropores formed by the destruction of the original zeolite skeleton.<sup>15</sup> This can explain why the maximum dehydration rate of the amorphized zeolites occurred at lower temperatures (<100 °C) than the maximum dehydration rate of the original (crystalline) zeolite powders (130 – 160 °C), as well as why water desorption from amorphized zeolites is higher (Fig. 5B) than the water desorption rate from the original crystalline samples (Fig. 5A).<sup>16</sup> However, a slower dehydration rate of the amorphized samples relative to the dehydration rate of the crystalline ones at  $T > 200$  °C (compare Figs 5A and 5B) is probably caused by blocking a part of the hydrated Na<sup>+</sup> ions in very small micropores (presumably, even smaller than the original channels and voids of the zeolite framework), formed by destroying the original crystal structure of zeolites.<sup>16</sup>

Assuming that the effective size of pores formed by destroying the original zeolite structure is considerably larger than the size of the hydrated cations, it is realistic to postulate that the size of the cation does not markedly affect the diffusion of desorbed water molecules through the pore system, and hence the dominant factor that controls the rate of dehydration is just the strength of the electrostatic force between the cation and the water molecules. An increase in the dehydration rate of the amorphized samples in the sequence:  $r_{d,Na,Li} < r_{d,Na} < r_{d,Na,K} < r_{d,Na,Cs}$  (see Fig. 5B), i.e. with the increase in the ionic radius of the exchanged ion ( $r_{Li^+} < r_{Na^+} < r_{K^+} < r_{Cs^+}$ ) corroborates such postulation.

Differential scanning calorimetry (DSC) of both original (crystalline) and amorphized zeolite A, showed appearance of exothermic peaks at  $T > 700$  (see Table 3).

The temperatures  $T_p(1)$  and  $T_p(2)$  for the amorphized sample of zeolite (Na, K)A are taken from the DSC curves of the crystalline sample because the amorphous sample has no exothermic peak.

The appearance of the exothermic peaks indicates the occurrence of solid-state transformation(s) of crystalline and amorphous phases into other crystalline and/or amorphous phases. Our previous investigation of the high-temperature, solid-state transformations of different types of zeolites<sup>14,32–38</sup> have shown that the thermal transformations may

Table 3 – Temperatures,  $T_p(n)$ , of the exothermic peaks in DSC curves of crystalline and amorphized samples of zeolite A in which a part of the original sodium ions has been exchanged by other ions.

Tablica 3 – Temperature  $T_p(n)$ , egzotermnih pikova u DSC-krivuljama kristalnih i amorfiziranih uzoraka zeolita A u kojima je dio natrijevih iona bio zamijenjen drugim ionima.

Zeolite Zeolit	Crystalline samples Kristalni uzorak			Amorphized samples Amorfizirani uzorci	
	$T_p(1)/^{\circ}\text{C}$	$T_p(2)/^{\circ}\text{C}$	$T_p(3)/^{\circ}\text{C}$	$T_p(1)/^{\circ}\text{C}$	$T_p(2)/^{\circ}\text{C}$
(Na,Li)A	760	822	1150	768	1150
NaA(4A)	899	1003	-	901	1118
(Na,K)A	962	1064	-	962*	1064*
(Na,Cs)A	1057	-	-	997	-
(Na,NH <sub>4</sub> )A	997	-	-	997	-
(Na,NH <sub>4</sub> )A	1000	-	-	1000	-

be divided into two steps: The first step is the formation of an amorphous phase by destroying the zeolite framework structure and the subsequent formation of a new crystalline non-zeolitic phase by its nucleation and crystal growth from the previously formed amorphous phase. The obtained crystalline phase depends on the type of zeolite precursors and on the cation(s) present in the precursors, while the stage of the transformation process depends on the temperature and time of heating.<sup>14,32–38</sup>

Analysis of the phase composition in the products obtained by heating at the DSC-peak temperatures (see Table 3) for different times (0.5–4h) of Li<sup>+</sup>, K<sup>+</sup>, Cs<sup>+</sup> and NH<sub>4</sub><sup>+</sup>-exchanged zeolite A, and the amorphous aluminosilicates obtained by ball – milling the crystalline precursors, have shown that the thermally induced transformations of the crystalline and amorphous precursors can be represented by the following transformation, Scheme 1.

Here the abbreviation ht = heating, bm = ball-milling, rt = room temperature. Am-bm = amorphous aluminosilicate obtained by ball-milling, and am-ht = amorphous aluminosilicate obtained by heating of zeolite.

As already stated, the first step of the thermal transformation of crystalline precursors (ion-exchanged zeolites) is the formation of an amorphous aluminosilicate phase by destroying the zeolite framework structure. Thermal stability of the zeolite framework, and thus the temperature of its transformation to the amorphous phase increases with the ionic radius of the alkali cations present in the channel-void system of the zeolite framework. Further transformation pathways of amorphous precursors formed by both heating and ball-milling of the starting crystalline phases, depend on the type of cation(s) present in the precursors: The presence of Na<sup>+</sup> ions favors the crystallization of carnegieite and nepheline with a tendency of further transformation of the thermodynamically unstable carnegieite to more stable nepheline at higher temperatures and/or prolonged heating time.

The presence of Li<sup>+</sup> ions favors the crystallization of  $\gamma$ -eucryptite at lower temperatures (760–822 °C) and  $\beta$ -eucryptite at higher temperatures (1150 °C).  $\gamma$ -Eucryptite

zeolite A	$\frac{\text{ht}}{800\text{ }^\circ\text{C}}$	$\text{NaAlSi}_3\text{O}_8$ <u>900 °C</u> Am-ht	$\Rightarrow \text{NaAlSi}_3\text{O}_8 \Rightarrow \text{NaAlSi}_3\text{O}_8$ carnegieite nepheline
	$\frac{\text{bm}}{\text{rt}}$	$\text{NaAlSi}_3\text{O}_8$ <u>900 °C</u> Am-bm	
			$\Rightarrow \text{LiAlSi}_3\text{O}_8$ $\gamma$ -eucryptite
	$\frac{\text{ht}}{>760\text{ }^\circ\text{C}}$	$(\text{Li,Na})\text{AlSi}_3\text{O}_8$ <u>760 °C-822 °C</u> Am-ht	
(Li,Na)A			$\Rightarrow (\text{Li,Na})\text{AlSi}_3\text{O}_8$ carnegieite
	$\frac{\text{bm}}{\text{rt}}$	$(\text{Li,Na})\text{AlSi}_3\text{O}_8$ <u>768 °C</u> Am-bm	$\Rightarrow \text{NaAlSi}_3\text{O}_8$ carnegieite $\Rightarrow \text{LiAlSi}_3\text{O}_8$ $\gamma$ -eucryptite $\Rightarrow \text{LiAlSi}_3\text{O}_8$ $\beta$ -eucryptite
			$\Rightarrow (\text{Li,Na})\text{AlSi}_3\text{O}_8$ $\gamma$ -eucryptite
			$\Rightarrow (\text{Li,Na})\text{AlSi}_3\text{O}_8$ $\beta$ -eucryptite
$(\text{Li,Na})\text{AlSi}_3\text{O}_8$ <u>1150 °C</u> Am-ht			
$(\text{Li,Na})\text{AlSi}_3\text{O}_8$ <u>1150 °C</u> Am-bm			$\Rightarrow (\text{Li,Na})\text{AlSi}_3\text{O}_8$ $\beta$ -eucryptite $\Rightarrow (\text{Li,Na})\text{AlSi}_3\text{O}_8 \Rightarrow (\text{Li,Na})\text{AlSi}_3\text{O}_8$ $\gamma$ -eucryptite $\beta$ -eucryptite $\Rightarrow \text{NaAlSi}_3\text{O}_8$ carnegieite
(Na,K)A	$\frac{\text{ht}}{960\text{ }^\circ\text{C}}$	$(\text{Na,K})\text{AlSi}_3\text{O}_8$ <u>&gt;960 °C</u> Am-ht	$\Rightarrow (\text{Na,K})\text{AlSi}_3\text{O}_8 \Rightarrow (\text{Na,K})\text{AlSi}_3\text{O}_8$ Kaliophilite Kalsilite
	$\frac{\text{bm}}{\text{rt}}$	$(\text{Na,K})\text{AlSi}_3\text{O}_8$ <u>&gt;960 °C</u> Am-bm	
(Na,Cs)A	$\frac{\text{ht}}{\text{ca. } 1000\text{ }^\circ\text{C}}$	$(\text{Na,Cs})\text{AlSi}_3\text{O}_8$ <u>ca. 1000 °C</u> Am-ht	$\Rightarrow \text{NaAlSi}_3\text{O}_8 \Rightarrow \text{NaAlSi}_3\text{O}_8$ carnegieite nepheline
	$\frac{\text{bm}}{\text{rt}}$	$(\text{Na,Cs})\text{AlSi}_3\text{O}_8$ <u>ca. 1000 °C</u> Am-bm	$\Rightarrow \text{CsAlSi}_3\text{O}_8, \text{NaAlSi}_3\text{O}_8$ pollucite
(Na,NH <sub>4</sub> )A	$\frac{\text{ht}}{1000\text{ }^\circ\text{C}}$	$0.21\text{Na}_2\text{O} \cdot \text{Al}_2\text{O}_3 \cdot 2\text{SiO}_2$ <u>1000 °C</u> Am-ht	$\Rightarrow 3\text{Al}_2\text{O}_3 \cdot 2\text{SiO}_2$ mullite
			$\Rightarrow \text{amorphous Na}_2\text{O} \cdot \text{SiO}_2$
	$\frac{\text{bm}}{\text{rt}}$	$(\text{Na,NH}_4)\text{AlSi}_3\text{O}_8$ <u>1000 °C</u> Am-bm	$\Rightarrow \text{amorphous SiO}_2$

S c h e m e 1 – “Reprinted from Publication printed in *Thermochimica acta*, 317, Authors: C. Kosanović, B. Subotić and I. Šmit, pages 25–37, Copyright (1997), with permission from Elsevier”.

S h e m a 1 – Prenešeno iz publikacije objavljene u *Thermochimica Acta*, **317**; Autori: C. Kosanović, B. Subotić, and I. Šmit, str. 25–37, Copyright 1997, uz dopuštenje Elseviera.

that may be formed at 1150 °C together with  $\beta$ -eucryptite, tends to transform into  $\beta$ -eucryptite at prolonged heating time. The formation of carnegieite at lower temperatures (760–822 °C) and the formation of nepheline at higher temperatures (1150 °C) is caused by the presence of Na<sup>+</sup> ions in the (Na,Li)-aluminosilicate precursors.

The presence of K<sup>+</sup> ions favors the crystallization of (Na,K)AlSi<sub>3</sub>O<sub>8</sub> of kaliophilite-type and its subsequent transformation into (Na,K)AlSi<sub>3</sub>O<sub>8</sub> of kalsilite type.

The presence of Cs<sup>+</sup> ions causes the crystallization of pollucite. The nepheline formed due to the presence of Na<sup>+</sup> ions in the (Na,Cs)-aluminosilicate precursors tends to transform into (Na,Cs)AlSi<sub>3</sub>O<sub>8</sub> of pollucite-type during the prolonged heating.

The amorphous precursor formed by both thermal treatment and ball-milling of the ammonium-exchanged zeolites A transforms at ca. 1000 °C to a mixture of mullite and an amorphous phase composed of Na<sub>2</sub>O · SiO<sub>2</sub> and SiO<sub>2</sub>.

The fraction of mullite in the product of heating is determined by the Al<sub>2</sub>O<sub>3</sub> content in the precursor while the fractions of Na<sub>2</sub>O · SiO<sub>2</sub> and SiO<sub>2</sub> are determined by the Na<sub>2</sub>O and SiO<sub>2</sub> content, respectively, in the precursor.

## Conclusion

The presented results lead to conclusion that ball-milling is an efficient method for the formation of amorphous aluminosilicate precursors with well defined composition and homogeneity.

Thermal treatment of such obtained precursors results in the crystallization of ceramic materials at temperatures much lower than needed for the formation of ceramics using crystalline aluminosilicates or adequate oxide mixtures as precursors.

Thermal treatment of the ion-exchange zeolite precursors (both crystalline and amorphized) results in the formation of different aluminosilicate-based ceramic materials.

Ceramic materials are formed through careful control of the nucleation and crystallization processes by thermal treatment of the prepared amorphous materials or by thermal treatment of the original crystalline zeolites through an intermediate amorphous phase to a crystalline nonzeolitic phase.

## ACKNOWLEDGEMENTS

The authors thank the Ministry of Science, Education and Sport of the Republic of Croatia for its financial support.

## References

### Literatura

1. D. W. Breck, *Zeolite Molecular Sieves*, Willy and Sons, New York, 1974.
2. E. M. Flanigen, in: Proc. Fifth Int. Conf. Zeolites, (Ed. L. V. C. Rees), Hayden, London-Philadelphia-Rheine, (1980) p. 764.
3. K. F. Fischer, W. M. Meier, *Fortschr. Miner* **42** (1965) 50.
4. D.W. Breck, *J. Chem. Educ* **41** (1964) 678.
5. R. M. Barrer, *Zeolites and Clay Minerals as Sorbents and Molecular Sieves*, Academic Press, 1978, p. 23.
6. W. H. Meier, D. H. Olson, *Atlas of Zeolite Structure Types*, Publ. by the Structure Commission of the International Zeolite Association, 1978.
7. W. Loewenstein, *Am. Mineral* **39** (1954) 92.

8. J. Cornier, J. M. Popa, M. Ubelmann, *L'actualite chimique*, 1992, 405.
9. D. E. W. Vaughan, *Chem. Eng. Progr.* (1988) 25.
10. D. E. W. Vaughan, in: *The Properties and Applications of Zeolites*, Special Publication No. 33 (Ed. R. P. Towsend), 1980, p. 294.
11. E. M. Flanigen, *Pure Appl. Chem.* **52** (1980) 2191.
12. M. A. Subramanian, D. R. Corbin, U. Chowdhry, *Bull. Mater. Sci.* **16** (1993) 665.
13. W. D. Kingery, H. K. Bowen, D. R. Uhlman, *Introduction to Ceramics*, 2<sup>nd</sup> Edition, Wiley, New York, 1976.
14. C. Kosanović, B. Subotić, E. Kranjc, *Microporous Mesoporous Mater.* **71** (2004) 27.
15. C. Kosanović, J. Bronić, B. Subotić, I. Šmit, M. Stubičar, A. Tonejc, T. Yamamoto, *Zeolites* **13** (1993) 261.
16. C. Kosanović, B. Subotić, A. Čižmek, *Thermochimica Acta* **276** (1996) 91.
17. C. Kosanović, J. Bronić, A. Čižmek, B. Subotić, I. Šmit, M. Stubičar, A. Tonejc, *Zeolites* **15** (3) (1995), 247.
18. C. Kosanović, A. Čižmek, B. Subotić, I. Šmit, M. Stubičar, A. Tonejc, *Zeolites* **15** (1) (1995) 51.
19. C. Kosanović, A. Čižmek, B. Subotić, I. Šmit, M. Stubičar, A. Tonejc, *Zeolites* **15** (1995) 632.
20. P. C. Borthakur, B. D. Chattaray, *J. Therm. Anal.* **17** (1979) 67.
21. A. J. Chandwadakar, S. B. Kulkarni, *J. Therm. Anal.* **19** (1980) 313.
22. B. L. Yu, A. Dyer, H. Enamy, *Thermochim. Acta* **200** (1992) 299.
23. R. C. Mackenzie, *Differential Thermal Analysis*, Vol.1, Academic Press, London, 1970, p. 498.
24. W. Smykatz-Kloss, *Differential Thermal Analysis, Application and Results in Mineralogy*, Springer-Verlag, Berlin, 1974, p. 81.
25. D. N. Todor, *Thermal Analysis of Minerals*, Abacus Press, Tunbridge Wells, Kent, UK, 1976, p. 208.
26. H. W. Haynes, *Catal. Rev. Sci. Eng.* **17** (1978) 283.
27. Z. Gabelica, J. B. Nagy, E. G. Deroane, J. P. Gilson, *Clay Minerals* **19** (1984) 803.
28. A. Aiello, F. Crea, A. Nastro, B. Subotić, F. Testa, *Zeolites* **11** (1991) 767.
29. Ramamurthy, D. R. Sanderson, D. F. Eaton, *Photochem. Photobiol.* **56** (1992) 297.
30. L. I. Antropov, *Theoretical Electrochemistry*, Mir Publishers, Moscow, 1972, p. 69.
31. P. K. Dutta, B. Del Barco, *J. Phys. Chem.* **108** (1986) 1861.
32. C. Kosanović, B. Subotić, I. Šmit, A. Čižmek, M. Stubičar, A. Tonejc, *J. Mat. Sci.* **32** (1996), 73.
33. C. Kosanović, B. Subotić, *Microporous Materials* **12** (1997) 261.
34. C. Kosanović, B. Subotić, V. Kaučić, M. Škrebilin, *Physical Chemistry Chemical Physics* **2** (2000) 3447.
35. C. Kosanović, B. Subotić, *Microporous Mesoporous Mater.* **66** (2003) 311.
36. C. Kosanović, B. Subotić, A. Ristić, *Chem. Mater.* **86** (2004) 390.
37. C. Kosanović, B. Subotić, A. Ristić, *Croat. Chem. Acta* **77** (2004) 553.
38. C. Kosanović, B. Subotić, I. Šmit, *Thermochimica Acta* **317** (1998) 25.

### List of symbols Popis simbola

a	– cell constant of zeolite, Å (10 <sup>-1</sup> nm) – konstanta jedinične ćelije zeolita, Å (10 <sup>-1</sup> nm)
c	– concentration, mol dm <sup>-3</sup> – koncentracija, mol dm <sup>-3</sup>
d	– diameter, mm – promjer, mm
f <sub>R</sub>	– fraction of cation R <sup>+</sup> – udjel kationa R <sup>+</sup>
k	– rate coefficient of amorphization, h <sup>-1</sup> – koeficijent brzine amorfizacije, h <sup>-1</sup>
l	– length, mm – duljina, mm
m	– mass, mg – masa, mg
n	– rotation speed, min <sup>-1</sup> – brzina rotacije, min <sup>-1</sup>
Q	– volume flow rate, cm <sup>3</sup> min <sup>-1</sup> – obujmni protok, cm <sup>3</sup> min <sup>-1</sup>
r <sub>a</sub>	– amorphization rate, h <sup>-1</sup> – brzina amorfizacije, h <sup>-1</sup>
r <sub>d</sub>	– dehydration rate, h <sup>-1</sup> – brzina dehidracije, h <sup>-1</sup>
r	– radius, mm – polumjer, mm
T	– temperature, °C – temperatura, °C
ΔT	– rate of temperature change, °C min <sup>-1</sup> – brzina temperaturne promjene, °C min <sup>-1</sup>
t	– time, h – vrijeme, h
V	– volume, mL – obujam, mL
w	– mass fraction – maseni udjel

**SAŽETAK****Mehanokemijske i termičke transformacije amorfnih i kristalnih alumosilikata***C. Kosanović i B. Subotić*

Priprava amorfnih alumosilikatnih prekursora definiranih svojstava bitan je čimbenik za studij nukleacije i kristalnog rasta zeolita tijekom njihovih termalnih i hidrotermalnih transformacija u zeolite i specijalne keramičke materijale. U ovom radu je prikazan učinak jakih mehaničkih sila na strukturalna svojstva zeolita A i zeolita A u kojem su  $\text{Na}^+$  ioni djelomično ili potpuno zamijenjeni različitim kationima ( $\text{Li}^+$ ,  $\text{K}^+$ ,  $\text{Cs}^+$ ,  $\text{NH}_4^+$ ).

Prikazan je utjecaj različitih kationa na mehaničku i termičku stabilnost zeolitne građe i dobivanje amorfnih prekursora kao i njihove termičke transformacije u nezeolitne kristalne faze.

*Institut Ruđer Bošković  
Bijenička 54, 10000 Zagreb, Hrvatska*

*Prispjelo 30. svibnja 2006.  
Prihvaćeno 7. rujna 2006.*